

## Development of Electrochemical Impedance Immunosensor for Sensitive Determination of Myoglobin

Xianhui Ren<sup>1</sup>, Yang Zhang<sup>1</sup>, Yuqi Sun<sup>1</sup> and Lili Gao<sup>2,\*</sup>

<sup>1</sup> The Second Affiliated Hospital to Mudanjiang Medical University, Mudanjiang, P.R. China

<sup>2</sup> Department of Clinical Laboratory, Hongqi Hospital, Mudanjiang Medical University, Aimin District, Mudanjiang 157011, China.

\*E-mail: [liligao\\_mmu@yeah.net](mailto:liligao_mmu@yeah.net)

Received: 9 February 2017 / Accepted: 25 May 2017 / Published: 12 July 2017

---

Effective bio-recognition element immobilization on the surface of the transducer is significantly important for fabricating an immunosensor. *Pithophora. Oedogonia*, a green algae, has been employed as the reducing agent in this study to accomplish the biosynthesis of Au nanoparticles. The whole procedure of synthesis occurred rapidly where Au nanoparticles were produced within 1 h after the reaction between Au salt and algal extract. Subsequently, electrochemical impedance myoglobin immunosensor was constructed using the obtained AuNPs. A wide detection range can be achieved from 0.02 to 1 $\mu$ M either in phosphate buffered saline or the whole serum, Furthermore, the as-fabricated immunosensors is potential to be utilised for the detection of myoglobin.

---

**Keywords:** *Pithophora. oedogonia*; Electrochemical impedance immunodetection; Myoglobin; Indium-tin-oxide; Acute myocardial infarction

### 1. INTRODUCTION

Recently, many researchers have been paying attention to the detecting clinical analytes of low concentrations. As for this aspect, the biosensors excel other conventional analytical approaches in their favourable efficiency and convenience. Generally, a self-contained transducer was combined with a biological interface in the biosensor. This combined mechanism could be selective and sensitive as soon as the analyte of interest was bound to it. A tethering layer facilitates the favourable immobilisation of the antibodies onto the transducer surface in several ways. Moreover, these antibodies are essential to the biological interface of an immunosensor [1, 2].

To determine protein biomarkers in the fields such as spectroscopy, electrochemistry, chromatography and colorimetric analysis, diverse immunoassays have been conducted according to

various signal-transduction principles in recent years [3-7]. As the most promising novel approach of these techniques, electrochemical detection is significantly sensitive, and could be fabricated with simple instrumentation with low cost [8, 9]. Based on previous studies, in order to endow (electrochemical impedance spectroscopy) EIS with preferable analytical traits, the following two issues should be paid attention to. Firstly, it is vital to construct a signal-generation label with great efficiency to amplify signals, thus obtaining a low limit of quantification and detection [10]. Besides, a significantly sensitive detection mode shall be utilized [11]. There has been a new era for the significant improvement of novel analytical tools and instrumentation, with the nanotechnology like the approaches of nanomaterials generation, manipulation and deployment increasingly studied [12, 13]. Under acidic conditions, anodic stripping voltammetric assay toward CdS quantum dots was adopted in an immunoassay conducted by Zhang and co-workers to detect IgG [14]. The detection limits are extremely low with stripping voltammetric detection which includes “built-in” preconcentration of great effectiveness. In this preconcentration process, the substrate is electroplated on the working electrode through deposition and oxidized from the electrode by stripping. In terms of stripping voltammetric detection, Au nanostructure has preferably been a perfect alternative since it is electronically active favorably and could be easily prepared. In order to detect genomic DNA sensitively, a hollow polyelectrolyte shell containing roughly  $1.0 \times 10^{11}$  Au atoms in the form of well dispersed Au nanoparticles has been designed by Khunrattanaorn and co-workers in their stripping voltammetric tag [15]. The stripping voltammetric monitoring of Au<sub>67</sub> nanoparticle label was reported by Pumera and co-workers as a novel electrochemical sensor to detect DNA hybridization [16]. EIS require being more sensitive in spite of these developments, thus it is essential to fabricate novel protocols. Featuring in non-destructive and sensitive performance in characterizing electrical traits in biological interfaces like interactions between oligonucleotides and DNAs and sensing formation of antigen–antibody and biotin–avidin complexes, the EIS has been popular among researchers in recent years [17, 18].

Through pre-diagnosis and treatment effect, the patients could possibly be managed in a better way, since there have been significantly more and more literatures concerning disease-related proteins as biomarkers [19, 20]. In the world scale, the diseases related to cardiovascular are among the most frequent death-causing diseases [21]. In 1h after acute myocardial infarction, myoglobin, a comparatively tiny protein molecule, is released to the blood. Note that this protein molecule could serve as a biomarker for heart attack in patients suffering chest pain. The peak of this release could be observed in 4-12 h, followed by a rapid elimination [22, 23]. Despite the filtration through kidneys, the resulting myoglobin is of toxicity to the renal tubular epithelium, thus acute the renal failure could be caused [24]. Myoglobin excels other cardiac biomarker candidates because acute myocardial infarction (AMI) could be detected at an earlier stage with the earlier release of myoglobin from damaged cells than its counterparts [25, 26]. Thus in clinically analysing AMI, it would be of great advantage to detect myoglobin with sensitiveness and accuracy. Herein, with the biosynthesized Au NPs, a platform is revealed to construct a bioelectrode to detect myoglobin, a cardiac biomarker, combining the merits of EIS approach and the traits of biosynthesized Au NPs which are covalently anchored on a 3-aminopropyltriethoxy silane (APTES) self assembled monolayer (SAM) over an indium-tin-oxide (ITO)-glass plate. Meanwhile, carbodiimide coupling reaction facilitates the attachment of Ab-

myoglobin (the cardiac protein antibody) to the carboxyl-functionalized AuNPs-modified APTES/ITO-glass plates. The obtained bioelectrode is indentified through diverse microscopic methods in a systematic way. In addition, with  $[\text{Fe}(\text{CN})_6]^{3-/4-}$  employed as a redox probe, its immunosensing capacity of quantitatively estimating Ag-myoglobin in phosphate buffer saline (PBS; pH 7.4) is studied with EIS.

## 2. EXPERIMENTS

### 2.1. Materials

The buffer solution adopted in the whole experiments conducted in the study was phosphate buffered saline (PBS) with  $\text{Na}_2\text{HPO}_4$  (0.1 mM),  $\text{KH}_2\text{PO}_4$  (1.8 mM), KCl (2.7 mM), and NaCl (140 mM), pH 7.2 with  $\text{K}_3[\text{Fe}(\text{CN})_6]/\text{K}_4[\text{Fe}(\text{CN})_6]$  (10 mM) in PBS taken as the redox mediator in proper conditions. 3-mercaptopropionic acid (MPA), 2-mercaptoethylamine (2-MEA) hydrochloride, horse heart myoglobin, and  $\text{HAuCl}_4$  were commercially available in Sigma-Aldrich Corp. *Pithophora oedogonia*, a green algae, was obtained in a fresh pond in Mudanjiang Medical University. Subsequently for the removal of extraneous impurity, Mill-Q water was adopted to wash fresh *Pithophora oedogonia*. The wet specimen went through 3 days drying in the shade, followed by complete drying in a 70°C oven. Through grounding treatment, the as-prepared *Pithophora oedogonia* specimen was finally presented in the form of fine powder for future application. At analytical grade, the rest chemicals were employed with no need of further purification.

### 2.2. AuNPs synthesis

To synthesize Au NPs, a mixture of water (100 mL) with *Pithophora oedogonia* powder (10 g) went through sonication for 15 min prior to 15 min of heating to 70 °C. Subsequently, filter paper with 200 nm pore was employed for the filtration of *Pithophora oedogonia* extract. The mixture of  $\text{HAuCl}_4$  solution (20 mL) and *Pithophora oedogonia* extract (20 mL) went through sonication for 1 h, thus producing Au nanoparticles. The as-prepared Au NPs was observed to be formed according to the resulting purplish yellow solution that had been originally light yellow. There were two steps in separation process: centrifugation at 10,000 rpm for 30 min and the wash cycle. The resulting Au NPs were put in a 70°C oven for drying. Subsequently a mixture of MPA (46  $\mu\text{L}$ ) with  $\text{H}_2\text{O}$  (10 mL) was rapidly added for the stabilization of as-prepared Au NPs solution, thus achieving functionalized Au NPs. The resulting mixture maintained at 50 mL was then stirred at ambient temperature for 2 h. The colloidal solution finally went through ethanol washing for 2 to 3 times, centrifugation at 20000 rpm, and drying for 12 h in vacuum.

### 2.3. Antibody purification

The purification of the anti-myoglobin IgG occurred on a protein G chromatography column balanced by  $\text{Na}_2\text{HPO}_4$  (20 mM), pH 7.0. The sample was then applied and allowed to flow through.

After washing with the same buffer, bound antibodies were eluted with 100 mM glycine-HCl, pH 2.7 into 1/10 volume of 1 M Tris-HCl, pH 9.5 to raise the pH to around pH 8.0. Dialysis of the eluate in 10 kDa cut off dialysis tubing was carried out overnight against 100 mM PBS, pH 7.4 at 4 °C. The diluted sample of IgG was then concentrated using an ultrafiltration unit (50 kDa cut off) and stored for further use.

#### 2.4. Immunosensor fabrication

After being ultrasonically cleaned, the ITO coated glass plates went through vacuum drying. In order for hydroxyl sheets to accumulate on the surface of ITO-glass, plasma chamber was employed to achieve the exposure of as-prepared ITO glass plates to oxygen plasma for 5 min. With spin coating scheme, a layer of bio-formed Au NPs covered ITO. After being dried, the electrodes went through de-ionised water rinsing for 3 times, followed by N<sub>2</sub> stream drying. An ethanolic solution of 4-aminothiophenol (4-ATP) (10 mM) was adopted for the immersion of Au electrodes cleaned a short time ago. The immersion was conducted at ambient temperature for 4 h. Subsequently ethanol was used for rinsing the as-prepared electrodes for several times prior to N<sub>2</sub> stream drying, which was followed by the immersion of the Au electrodes modified by 4-ATP SAM to 5 mM sulfosuccinimidyl 4-[N-maleimidomethyl]cyclohexane-1-carboxylate (sulfo-SMCC) solution in PBS-EDTA, pH 7.2 at ambient temperature for 1 h. Then a PBS-EDTA, pH 7.2 buffer was utilized for rinsing the modified surface of as-incubated electrodes, followed by compressed N<sub>2</sub> drying, thus activating the electrodes which could either be immediately utilized or put into storage at 4 °C in desiccation for future application. The application of freshly formed half-antibody fragment solution to the surface of as-prepared Au electrode lasted 2 h. PBS-EDTA with the pH of 7.2 was subsequently employed for a complete wash of as-prepared electrodes, with no unbound antibody fragments left. Then N<sub>2</sub> stream drying was conducted for them. Before and after the addition of analyte, electrochemical assessments were employed to assay as-prepared electrodes.

#### 2.5 ELISA determination

Microtiter plates were coated with antibody by incubation at 4 °C for 16 h with 6 µg/mL antibody in borate buffer, 200 µL being applied to each well. Temperature variation was minimized by placing the plate in a small enclosed box in a cold room at 4°C. The plate wells were washed once with 200 µL of PBS-Tween reagent. 8 mM/L disodium hydrogen phosphate and 137 mM/L sodium chloride containing 500 µL of Tween 20 per L. A stock myoglobin standard of 1024 µL was prepared by diluting a purified preparation containing 2 µg/mL in PBS reagent and 100 mL chicken serum per L and the portions stored at -20°C until required. Standards were assayed in triplicate and samples in duplicate by adding 100 µL to wells, placing the microtiter plate in a small closed container and incubating for 2 h at room temperature. The plates were washed twice with 200 µL of PBS-Tween reagent delivered with a multi pipette and blotted briefly by inversion on paper-towelling between ejection of antigen solution and washes. After washing, 150 µL of PBS Tween reagent containing 0.6 µg/mL of horseradish peroxidase-conjugated rabbit antibody to human myoglobin was added to each

well. The plate was then placed in a small closed container and incubated for 1 h at room temperature. After incubation, the plates were washed 6 times as previously described with the plate being rotated horizontally through 180° after each wash. To each well 100  $\mu\text{L}$  of substrate consisting of 3.7 mM/L o-phenylenediamine and 5 mM/L hydrogen peroxide in 34.7 mmol/L citric acid, 66.7 mM/L disodium hydrogen phosphate buffer, pH 5.0, was then added. Colour was allowed to develop for 30 min at room temperature and the reaction then stopped by addition of 100  $\mu\text{L}$  of 2.5 M/L  $\text{H}_2\text{SO}_4$  with the absorbance being measured at 495 nm with a Titertek Multiscan MCC/340 plate reader (Flow Laboratories). A sample blank was obtained using diluted chick serum and a colour reagent blank was obtained by omitting sample, standard and antibody.

### 3. RESULTS AND DISCUSSION

Upon the addition of the *Pithophora oedogonia* extract to  $\text{HAuCl}_3$  solution, the biosynthesis reaction in the experiment began. The Au NPs was observed to be nucleated with the dispersion gradually becoming purplish yellow from light yellow. Light at certain wavelength could be absorbed by the scattered metallic nanoparticle. In this way, in the as-prepared Au NPs dispersion, the surface plasmon resonances of the Au NPs would be monitored. Note that several elements such as size, solvent and morphology would influence the optical trait of Au NPs. *Pithophora oedogonia* was employed to construct Au NPs whose UV-vis spectrum is indicated in Figure 1A. At 551 nm of the spectrum, there is an obvious absorption peak, which coincides with the surface plasmon resonance of the Au NPs. This reveals that metallic Au material has been formed. The as-formed Au NPs could have the mean size revealed through the location of surface plasmon resonance peak. Based on previous studies, it could be predicted that the size of as-biosynthesized AuNPs ranges between 20 and 80 nm with scanning electron microscopy (SEM). Figure 1B reveals the spherical shape with tiny aggregation of as-biosynthesized Au NPs. Herein it could be indicated that the size of as-synthesized gold NPs through *Pithophora oedogonia* was likely to be uniform.

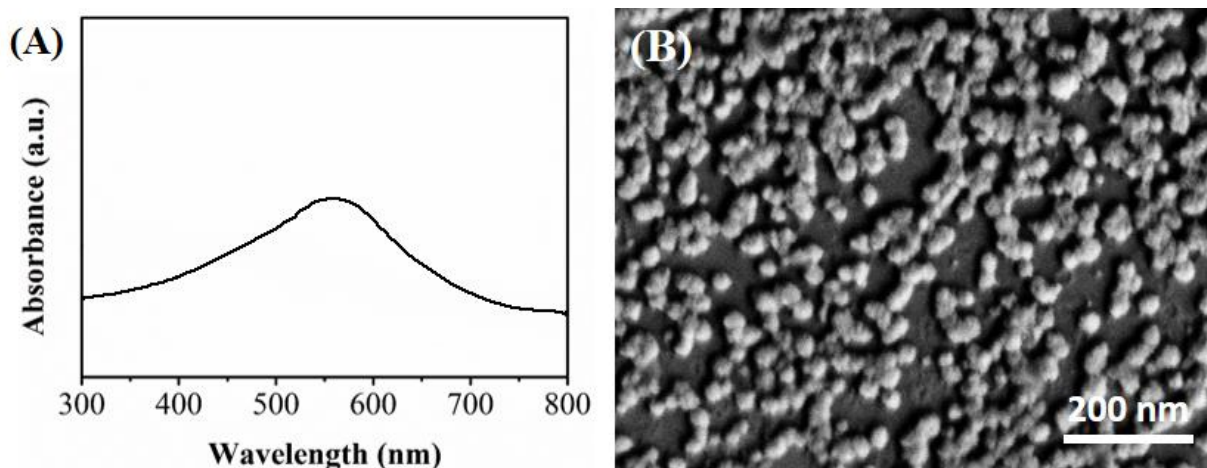


**Figure 1.** (A) UV-vis spectrum and (B) SEM pattern of biosynthesized AuNPs.

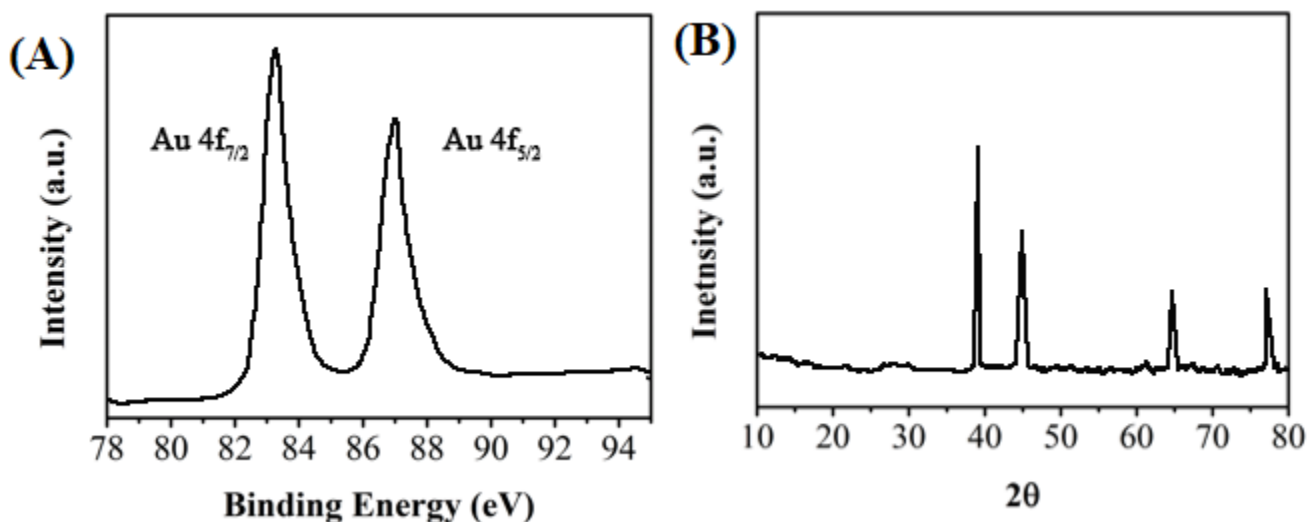


**Figure 2.** (A) High resolution Au 4f scan and (B) XRD image of the bioformed Au nanoparticles.

X-ray photoelectron spectroscopy (XPS) was another approach to confirming that Au NPs had been synthesized. The Au<sub>4f</sub> high resolution XPS scan of as-formed Au NPs is manifested in Figure 2A, with Au<sub>4f 7/2</sub> peaks observed on the 83.5 eV and Au<sub>4f 5/2</sub> peaks on 87.2 eV [27, 28]. The biomolecules of *Pithophora oedogonia* extract was attached to the surface of Au NPs, which led to a peaks transfer of Au<sup>0</sup> at 84.0 and 87.7 eV. As indicated from Figure 2B, XRD spectrum of as-synthesized AuNPs reveals diffraction peaks at 39.3°, 45.9°, 67.7° and 81.9°, which coincide with (111), (200), (220) and (311) planes of face-centered-cubic (fcc) crystallographic structure of Au (JCPDS 4-0783), respectively. The metallic Au material was also proved to have been synthesized by the result of XRD.

The capacity of measuring the property of monolayer films is a remarkable advantage of Cyclic voltammetry (CV). These films would impede the shift reactions at the interface of electrolyte and the electrode modified by SAM. Note that in this blocking mechanism, a redox couple was employed as a probe molecule. The CVs of an original Au electrode were revealed in Figure 3, together with the modification processes in [Fe(CN)<sub>6</sub>]<sup>3-/4-</sup> aqueous electrolyte system with a potential scan rate (50 mV/s). CVs of 4-ATP SAM on Au electrode can also be observed in Figure 3, in addition to those of deposited half-antibody fragments on the as-prepared electrode. It revealed a diffusion-limited reaction for electron shift for the original electrode, which was reflected by a reversible peak of Au electrode for the redox couple [Fe(CN)<sub>6</sub>]<sup>3-/4-</sup>. The peak-to-peak potential separation ( $\Delta E_p$ ) was about 50 mV at and the ratio of the redox peak current  $I_{pa}/I_{pc}$  was about 1 suggesting that the electrochemical reaction is reversible as a result of the construction of the AuNPs and the small peak-to-peak separation indicated a fast electron transfer rate [29]. However, it can be proposed that the electron shift was impeded for redox reaction as for electrode modified by 4-ATP SAM, which was supported by no appearance of obvious peak. Figure 3 indicates that a significant separation for current can be monitored in a curve of for 4-ATP SAM when forward scan ends and reverse scan begins. This separation reveals a mild obstruction by monolayer film. It can also be proposed from these CVs that the redox groups have been offered great convenience for radical diffusion, because ions can go through the pinholes and pores in SAM, which can be seen as microelectrode array traits. On the

contrary, for the original Au electrode, the monitored diffusion type was linear. Note that there was a radical blocking for electron shift after the half-antibody fragments were covalently immobilized onto Au electrode modified by 4-ATP.

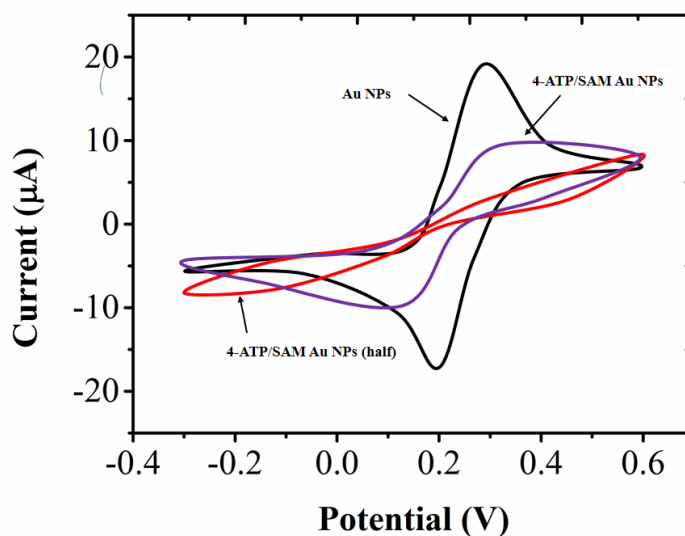


**Figure 3.** CV of an original Au electrode and SAMs onto it, indicating current ( $I/\mu\text{A}$ ) as a function of potential in 10 mM  $\text{K}_3\text{Fe}(\text{CN})_6/\text{K}_4\text{Fe}(\text{CN})_6$  in PBS with a pH of 7.0 and a scan rate of 50 mV/s.

As for the characterization of materials and surface interfaces, researchers usually refer to EIS which tops the rank of electro-analytical methods. In theory, either simplified or linearised current–potential traits can be applied for the analysis of responses as for EIS, since it just need a slight amplitude perturbation from the steady state, for which EIS excels other candidates. The range for impedance assessments was between 25 kHz and 0.25 Hz. Figure 4 reveals the complex impedance plots. There are generally two patterns in the impedance spectra: the compressed semicircle part and the linear portion. Specifically, the compressed semicircle part coinciding with limited electron shift was monitored at higher frequencies. In contrast, the linear portion coinciding with the diffusion limited electron shift occurred at comparatively lower frequencies. It can be proposed that the spectra were similar to those of Randle's equivalent circuit in theory. In Nyquist plots the diameters of the semicircles rose, which was reflected through the impedance spectra of complete immunosensor and electrode modified by 4-ATP SAM. The real component of impedance ( $Z'$ ) generally indicates electron transfer resistance ( $R_{\text{ct}}$ ) which has been observed to be favorable than capacitive changes. Moreover, the responses of the antibody–antigen interaction are most desirably reflected by the real component of impedance ( $Z'$ ) in sensitiveness and directness. Despite the possible similar performance of the imaginary component ( $-Z''$ ) (not shown), this work employed the real component of the impedance as the sensor signal to recognize analyte. When self-assembly of 4-ATP and antibody on the Au electrode was accomplished,  $R_{\text{ct}}$  was observed to be 447.4 and 305.2  $\Omega$  in order. The decline in the value of  $R_{\text{ct}}$  showed that adding 4-ATP remarkably shifted the reactivity, resulting in more physical or chemical interaction [30].

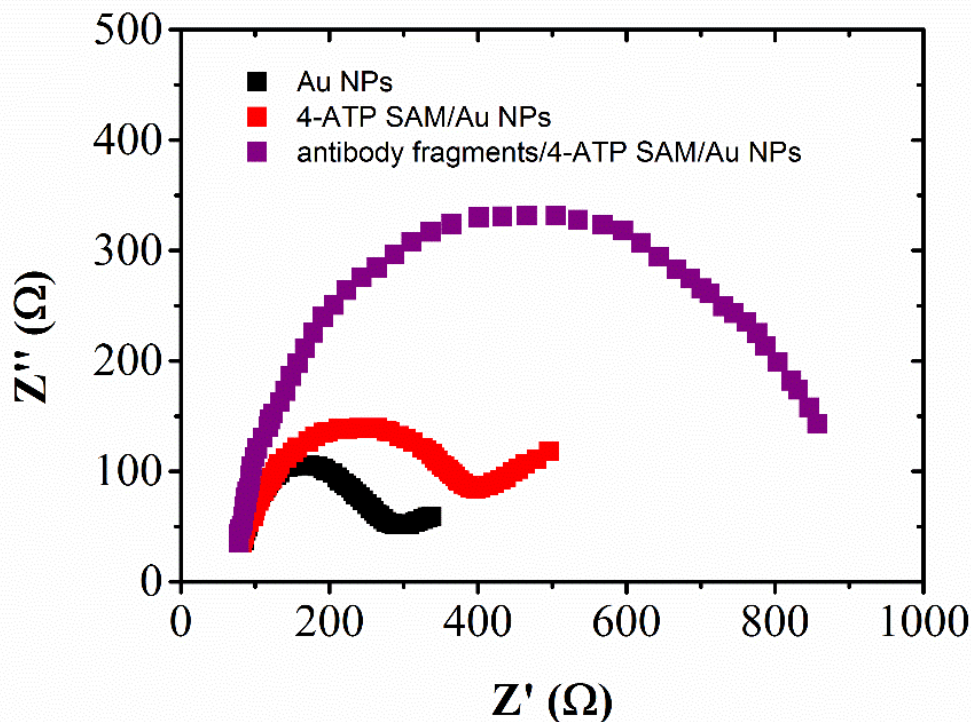


**Figure 4.** Nyquist plots of impedance spectra following sequential immobilization steps onto Au electrodes towards functional immunosensors. A function of the practical component ( $Z'/M\Omega$ ) is the imaginary component of impedance ( $-Z''/M\Omega$ ). Impedance spectra were recorded in 10 mM  $K_3Fe(CN)_6/K_4Fe(CN)_6$  in PBS, pH 7.0 with frequency in the range between 25 KHz and 250 mHz: (a) bare Au electrode, (b) 4-ATP SAM/Au electrode, and (c) antibody fragments/4-ATP SAM/Au electrode with bias potential of 0.4 V vs. Ag/AgCl reference electrode and the amplitude of the alternating voltage was 10 mV.

Non-Faradaic impedance biosensors perform impedance measurement in the absence of any redox probe. Bacteria detection is based on the impedance change upon the attachment of bacterial cells on an interdigitated microelectrode in the absence of any redox probe in the sample solution [31]. The antibody–antigen complex is formed after Ag-myoglobin at the surface of the electrode immunoreacts specifically with its complimentary target, Ab-myoglobin. The electron transfer was interrupted between the solution and bioelectrode due to a kinetic barrier caused by as-formed complex. There is a drop for capacitance with rising electron transfer resistance which results from growingly impeded Faradaic reaction of a redox couple. The control sample refers to the solution with no Ag-myoglobin (target protein). The response of it is revealed by  $R_{et}$  value correspondingly. After the target protein antigen of various concentrations being added continuously in equal portions, there was a different pattern for Nyquist plots indicated in Figure 5. Because of the interaction between antigen and antibody, as the Ag-myoglobin being added rises in concentration, an increase can be observed for the diameter of Nyquist circles.  $Y_0$  has been also observed to reduce, which corresponds to reduced capacitive performance of bioelectrode with immunoreactions.

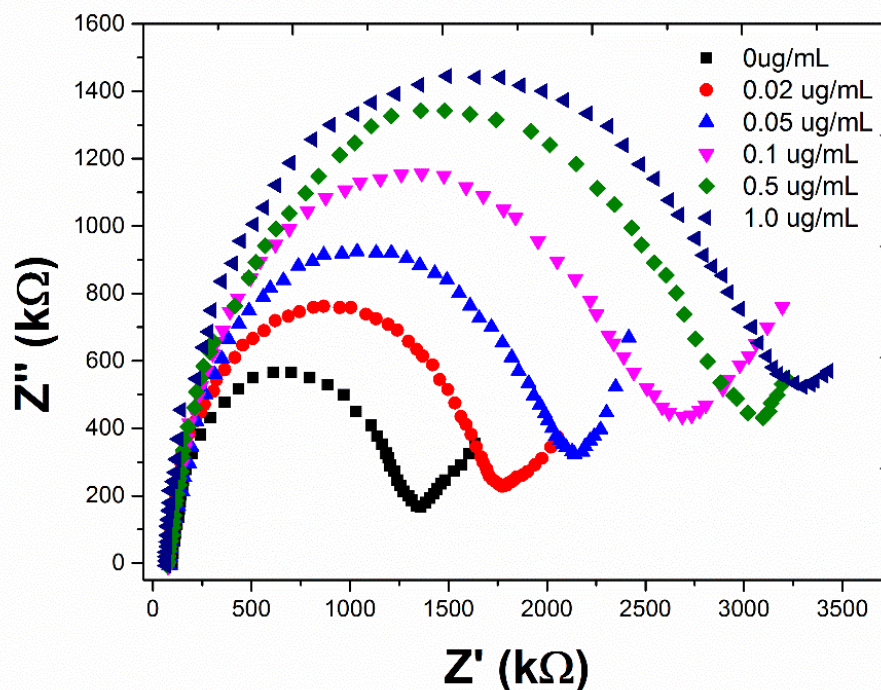


**Figure 5.** Faradaic impedance spectra of the antibody fragments/4-ATP SAM/Au electrode for various concentrations of myoglobin in PBS (pH 7.4) with 0.1 M KCl solution containing 2 mM  $[\text{Fe}(\text{CN})_6]^{3-/4-}$ .

In Figure 6, the change in the logarithmic value of Ag-myoglobin concentration ranging 20 ng/mL to 1  $\mu\text{g/mL}$  against the specific electron charge transfer resistance ( $\Delta R_{\text{et}} = (R_{\text{et}})_{\text{after immunoreaction}} - (R_{\text{et}})_{\text{control}}$ ) was observed to be plotted, thus achieving the sensitivity of as-constructed bioelectrode. The detection limit was obtained as 5.5 ng/mL, triple the signal-to-noise ratio. The sensitivity of the proposed sensor was compared with that of other reported myoglobin sensors and the results were presented in Table 1. In comparison to ELISA which needs several days to be conducted, the whole measurement as for EIS experimental procedure only lasts around 12 min, a quarter of which is allocated to preparing samples with no early treatment. This advantage means that EIS is promising to be applied to detect AMI at an early stage. Due to its advantages of advanced sensitivity, simplest preparation and stages in experiment, and physiological range for detecting myoglobin, it can be proposed that as-prepared bioelectrode excels its lately issued counterparts concerning carbon/ metal nanoparticle/semiconductor nanomaterials as well as myoglobin sensors based on complex. The proposed electrode remain 93% of its initial current response to myoglobin after 4 weeks storage, indicating the electrochemical sensor has the good stability. The reproducibility was examined at five modified electrodes prepared in the same conditions and a relative standard deviation (RSD) of 5.1% was obtained. The RSD of the response to 0.1 mM myoglobin was 5.2% for 6 successive measurements, indicating the electrochemical sensor has the good repeatability. The influence of various potentially interfering substances for determination of 0.1 Mm myoglobin was studied The results indicated that 20-fold of  $\text{Zn}^{2+}$ ,  $\text{Cu}^{2+}$ ,  $\text{SO}_4^{2-}$ , glucose, sucrose and amyllum, ascorbic acid and uric

acid had almost no influence on the determination and the tolerance limit was estimated to be less than 6% of the relative error.

To evaluate the applicability of the proposed assay, the designed electrochemical sensor was applied to measure myoglobin in human serum. Known concentrations of myoglobin were spiked into serum. The serum samples were diluted 10 times, followed by measuring the concentration of myoglobin using the designed sensing method. The recoveries for myoglobin in human serum samples were in the range of 90.8–103.4% with relative standard deviations between 2.7% and 4.4%, suggesting the developed sensor could be utilized to precisely detect myoglobin in complex biological samples.

**Table 1.** Comparison of the present sensor with other electrochemical myoglobin sensors.

Electrode	Linear range	Detection limit	Reference
Metal nanoparticles /didodecyldimethylammonium bromide	0.3 to 10 $\mu\text{g/mL}$	50 ng/mL	[32]
Graphene–ionic liquid–chitosan	1 to 5 $\mu\text{g/mL}$	0.2 $\mu\text{g/mL}$	[33]
Chitosan/hyaluronic acid	0.5 to 2 $\mu\text{g/mL}$	20 ng/mL	[34]
Methylene blue-multiwalled carbon nanotubes	0.1 to 3 $\mu\text{g/mL}$	5 ng/nL	[29]
Antibody fragments/4-ATP SAM/Au	0.02 to 1 $\mu\text{g/mL}$	5.5 ng/mL	This work

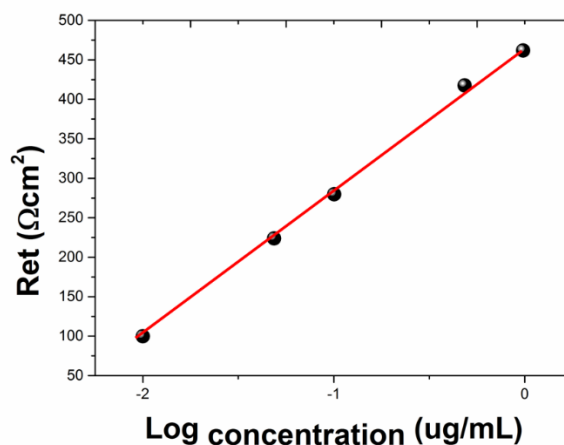


**Figure 6.** Concentration dependent calibration curve of the bioelectrode.

#### 4. CONCLUSIONS

This work reported a biosynthesis approach to preparing Au NPs with *Pithophora oedogonia* adopted as the reducing agent. Meanwhile, it featured a novel monolayer which can be self-assembled. As for the monolayer, there was targeted cross link of half antibodies to its base layer (4-

aminothiophenol). In terms of this mechanism, pretty moderate reduction with 2-MEA resulted in the cleavage of complete IgG, thus leading to the manifestation of the distinctive cysteine thiols. With their immobilization on the surface of the immunosensor, the pairing up of the half antibodies occurs and interrupted by with the addition of myoglobin analyte, revealing the targeted mobilization. The as-prepared biosensor is potential to be applied for the diagnosis of acute myocardial infarction.

## References

1. D. Tang, B. Su, J. Tang, J. Ren and G. Chen, *Anal. Chem.*, 82 (2010) 1527.
2. B. Zhang, Y. He, B. Liu and D. Tang, *Anal. Chim. Acta.*, 851 (2014) 49.
3. Y. Lin, Q. Zhou, Y. Lin, M. Lu and D. Tang, *Anal. Chim. Acta.*, 887 (2015) 67.
4. V. Kumar, S. Agarwal, D. Sharma, K.K. Sharma and D. Dwivedi, *Advanced Science Letters*, 20 (2014) 1723.
5. S.K. Mishra, A.K. Srivastava and D. Kumar, *RSC Advances*, 4 (2014) 21267.
6. J. Zhu, N. Zou, H. Mao, P. Wang, D. Zhu, H. Ji, H. Cong, C. Sun, H. Wang and F. Zhang, *Biosensors and Bioelectronics*, 42 (2013) 522.
7. K.A. Edwards, K.J. Meyers, B. Leonard and A.J. Baeumner, *Anal Bioanal Chem*, 405 (2013) 4017.
8. J. Tang, D. Tang, R. Niessner, G. Chen and D. Knopp, *Anal. Chem.*, 83 (2011) 5407.
9. Z. Zhong, M. Li, Y. Qing, N. Dai, W. Guan, W. Liang and D. Wang, *The Analyst*, 139 (2014) 6563.
10. X. Pei, B. Zhang, J. Tang, B. Liu, W. Lai and D. Tang, *Anal. Chim. Acta.*, 758 (2013) 1.
11. D. Tang, Y. Cui and G. Chen, *The Analyst*, 138 (2013) 981.
12. D. Knopp, D. Tang and R. Niessner, *Anal. Chim. Acta.*, 647 (2009) 14.
13. L. Wang and G. Arrabito, *The Analyst*, 140 (2015) 5821.
14. B. Zhang, D. Tang, I.Y. Goryacheva, R. Niessner and D. Knopp, *Chemistry—A European Journal*, 19 (2013) 2496.
15. N. Khunrattanaporn, P. Rijiravanich, M. Somasundrum and W. Surareungchai, *Biosensors and Bioelectronics*, 73 (2015) 181.
16. M. Pumera, M.T. Castaneda, M.I. Pividori, R. Eritja, A. Merkoçi and S. Alegret, *Langmuir*, 21 (2005) 9625.
17. A. Venkatanarayanan, T.E. Keyes and R.J. Forster, *Anal. Chem.*, 85 (2013) 2216.
18. S. Shrikrishnan, K. Sankaran and V. Lakshminarayanan, *J Phys Chem C*, 116 (2012) 16030.
19. E. Emilia and P. Neelakantan, *Journal of Clinical Pediatric Dentistry*, 39 (2015) 94.
20. Y. Li, J. Liang and P. Hou, *Clinica Chimica Acta*, 448 (2015) 124.
21. M. Di Pietro, S. Filardo, F. De Santis, P. Mastromarino and R. Sessa, *International journal of molecular sciences*, 16 (2014) 724.
22. V. Kumar, M. Shorie, A.K. Ganguli and P. Sabherwal, *Biosensors and Bioelectronics*, 72 (2015) 56.
23. Q. Wang, L. Liu, X. Yang, K. Wang, N. Chen, C. Zhou, B. Luo and S. Du, *Anal. Chem.*, 87 (2015) 2242.
24. H.Y. Lee, J.S. Choi, P. Guruprasath, B.-H. Lee and Y.W. Cho, *Analytical Sciences*, 31 (2015) 699.
25. M. Shorie, V. Kumar, P. Sabherwal and A. Ganguli, *CURRENT SCIENCE*, 108 (2015) 1595.
26. Q. Wang, F. Liu, X. Yang, K. Wang, H. Wang and X. Deng, *Biosensors and Bioelectronics*, 64 (2015) 161.
27. R. Leppelt, B. Schumacher, V. Plzak, M. Kinne and R. Behm, *J. Catal.*, 244 (2006) 137.
28. J. Li, C.-y. Liu and Y. Liu, *Journal of Materials Chemistry*, 22 (2012) 8426.
29. S. Pakapongpan, R. Palangsantikul and W. Surareungchai, *Electrochimica Acta*, 56 (2011) 6831.
30. S.K. Mishra, D. Kumar and A.M. Biradar, *Bioelectrochemistry*, 88 (2012) 118.
31. S.M. Radke and E.C. Alocilja, *Biosensors & bioelectronics*, 20 (2005) 1662.
32. E.V. Suprun, A.L. Shilovskaya, A.V. Lisitsa, T.V. Bulko, V.V. Shumyantseva and A.I. Archakov,

*Electroanalysis*, 23 (2011) 1051.

33. C. Ruan, T. Li, Q. Niu, M. Lu, J. Lou, W. Gao and W. Sun, *Electrochimica Acta*, 64 (2012) 183.

34. H. Lu and N. Hu, *J Phys Chem B*, 110 (2006) 23710.

© 2017 The Authors. Published by ESG ([www.electrochemsci.org](http://www.electrochemsci.org)). This article is an open access article distributed under the terms and conditions of the Creative Commons Attribution license (<http://creativecommons.org/licenses/by/4.0/>).